

# Morphology and Mechanical Properties of Injection-Molded Ultrahigh Molecular Weight Polyethylene/Polypropylene Blends and Comparison with Compression Molding

Meiju Xie,<sup>1,2</sup> Jinyao Chen,<sup>1</sup> Huilin Li<sup>1</sup>

<sup>1</sup>The State Key Laboratory of Polymer Materials Engineering, Polymer Research Institute of Sichuan University, Chengdu, Sichuan 610065, People's Republic of China

<sup>2</sup>Analytical and Testing Center, Sichuan University, Chengdu 610064, People's Republic of China

Received 3 January 2008; accepted 9 June 2008

DOI 10.1002/app.29036

Published online 17 October 2008 in Wiley InterScience (www.interscience.wiley.com).

**ABSTRACT:** The mechanical properties and morphology of UHMWPE/PP(80/20) blend molded by injection and compression-molding were investigated comparatively. The results showed that the injection-molded part had obviously higher Young's modulus and yield strength, and much lower elongation at break and impact strength, than compression-molded one. A skin-core structure was formed during injection molding in which UHMWPE particles elongated highly in the skin and the orientation was much weakened in the core. In the compression-molded part, the phase morphology was isotropic from the skin to the core section. The difference in consolidation degree

between two molded parts that the compression molded part consolidated better than the injection one was also clearly shown. In addition, compositional analysis revealed that there was more PP in the skin than core for the injection-molded part, whereas opposite case occurred to the compression-molded one. All these factors together accounted for the different behavior in mechanical properties for two molded parts. © 2008 Wiley Periodicals, Inc. *J Appl Polym Sci* 111: 890–898, 2009

**Key words:** UHMWPE/PP blends; morphology; mechanical properties; injection molding

## INTRODUCTION

Ultrahigh molecular weight polyethylene (UHMWPE) is applicable in various fields because of a set of technically important properties including high notched impact strength, low friction coefficient, and high wear resistance. However, at this high molecular weight, UHMWPE has pronounced viscoelastic characteristics in the melt, namely, extremely high viscosity and very low critical shear rate, which makes it unsuitable for conventional processing operations except for compression molding and ram extrusion. Numerous efforts have been made to reduce the melt viscosity.<sup>1–6</sup> Among them, blending with proper amount of polypropylene (PP)

(10 ~ 20 phr) was proved to be an effective way, which not only improved the rheological properties but also maintained the impact strength and abrasion resistance of UHMWPE.<sup>4,7,8</sup> UHMWPE/PP blend can thus be molded by general single screw extrusion. The addition of small amount of poly(ethylene glycol) (PEG) additives (PEG and its hybrids with inorganic fillers) could improve the processability of UHMWPE/PP blend further, resulting in significant reduction of the melt viscosity and obvious increase of the flow rate at a given die pressure during extrusion.<sup>9,10</sup> Such modification also made possible that UHMWPE was molded by conventional injection.

The final part prepared by different molding operation usually exhibits different morphological characteristics, which in turn is influential to the mechanical properties. Ghiam and White<sup>11</sup> have studied the development of phase morphology in injection and compression molding of nylon-6(PA6)/polyethylene(PE) blends. The phase morphology of the compression-molded part was isotropic, while that of both screw and ram injection-molded parts was both heterogeneous and anisotropic through the cross section. In the injection-molded parts, the morphology exhibited its greatest level of isotropy in the

Correspondence to: H. Li (nic7703@scu.edu.cn).

Contract grant sponsor: National Nature Science Foundation of China; contract grant number: 50233010.

Contract grant sponsor: National Basic Research Program of China; contract grant number: 2005CB623800

Contract grant sponsors: Foundation of Doctoral Disciplines and Ministry of Education of China; contract grant number: 20030610057.

*Journal of Applied Polymer Science*, Vol. 111, 890–898 (2009)  
© 2008 Wiley Periodicals, Inc.

core and became increasingly anisotropic approaching the mold wall. Similar injection molding-induced skin-core structure was also found in PP blends modified with ethylene/propylene/diene terpolymer and thermoplastic polyolefin rubber,<sup>12</sup> poly(ethylene terephthalate)(PET)/PE, and polycarbonate(PC)/PE blends.<sup>13</sup> Fellahi et al.<sup>14</sup> have compared the tensile properties of PP/PC blends obtained by injection molding and compression molding. Owing to flow induced dispersed phase orientation in injection molding, the tensile strength and modulus of injection-molded specimens were higher than those of compression-molded specimens.

As for UHMWPE, the structure developed in compression molding or ram extrusion and its relation with properties have been studied widely. It is difficult to achieve complete consolidation and homogenization in UHMWPE material, even in the relatively slow process of compression molding and ram extrusion.<sup>15–20</sup> The processed material usually exhibits fusion defects (particle boundaries) more or less. Farrar and Brain<sup>16</sup> reported that after ram-extrusion of the resin, the polymer retained some “memory” of the original powder particles at the 100  $\mu\text{m}$  scale. In compression-molding of UHMWPE, the varying time and temperature in the melt state during processing had dominant effect on the consolidation of the molded part.<sup>18,19</sup> Wu et al.<sup>18</sup> showed that the severity of the fusion defects reduced with increasing temperature and dwell time leading dramatic rise in elongation to break. An increase in pressure applied at melt was found to increase the polymer crystallinity and consolidation until a certain critical pressure was reached, while an increase in pressure applied at the recrystallization temperature caused a steady increase in the crystallinity and stiffness.<sup>20</sup> Compaction process on solid state (at a temperature close to, but lower than, the melting point of the reactor powder) is an effective way to achieve UHMWPE material with high toughness. Gao et al.<sup>21</sup> reported that recrystallization and re-entanglement processes occurred at the particle boundaries during compaction, and an optimum compaction pressure existed for the compacted precursors to retain maximum chain mobility and produce the maximum mechanical toughness. UHMWPE processed by high velocity compaction (HVC) reveals to be ductile and exhibits higher Young's modulus and yield stress than conventionally processed UHMWPE.<sup>22</sup> HVC UHMWPE can be seen as a bi-phased material of nascent and recrystallized UHMWPE at the micrometric scale. Low recrystallized phase fraction favors the stiffness at the cost of ultimate properties, whereas high recrystallized phase fraction favors the ultimate properties at the cost of stiffness. Mechanical properties are hence adjustable according to a given application.

However, the study on the injection-molded UHMWPE was rare because the unmodified UHMWPE can hardly be injection-molded unless at very high pressure.<sup>23</sup> Blending with PP and PEG additives provided a way for UHMWPE to be molded by conventional injection molding and gave injection-molded examples for comparative study. In this article, an experimental investigation of phase morphology formed in injection and compression molding of UHMWPE/PP blends and its relation with mechanical properties were presented.

## EXPERIMENTAL

### Materials

UHMWPE (M-II) and PP (F401) were two kinds of raw material used in this study. UHMWPE (M-II) was supplied by Beijing No.2 Auxiliary Agent Factory with an average molecular weight of  $2.5 \times 10^6$  and a mean particle diameter of about 300  $\mu\text{m}$ . PP (F401) was supplied by Lanzhou Chemical Industry Factory with a MFR of 2.0 g/10 min (230°C, 2.16 kg load). Poly(ethylene glycol) (PEG) additives included PEG and PEG/diatomite hybrid. PEG was supplied by Aoke Chemical limited company, Liaoyang, China, with an average molecular weight of 6000. Diatomite was supplied by Nahui desiccating agent company, Shanghai, China. Its average particle size was 5  $\mu\text{m}$ . To prepare the hybrid, PEG and diatomite with weight ratio of 1/2 were first blended in a two-roll mill then pulverized. In addition, Irganox1010 (Ciba,USA) was also used as antioxidant.

### Blending

The UHMWPE/PP blends were prepared as follows. UHMWPE and PP with weight ratio of 80/20 were mixed with or without a small amount of PEG additives in a high speed mixer. Ten minutes later, the mixture was compounded using a corotation Haake Record 90 (Bersdorff, Germany) twin-screw extruder. The barrel temperatures were 190, 210, and 215°C for the back, middle, and front section, respectively, and the die temperature was 210°C. The screw rotation speed was 30 rpm. The extrudate was palletized into granules.

### Injection molding

UHMWPE/PP(80/20) blend bars (as seen in Fig. 1) for mechanical test were molded on a Milacron K-TEC40 reciprocating screw injection-molding machine. Samples were produced using a two-cavity mold with a single gate in the end of each cavity. The mold temperature was set at 60°C. The temperature for the back, middle, and front section of the



**Figure 1** Schematic diagram of the injection-molded bars for mechanical test. (Left, bar for tensile test; Right, bar for impact test).

screw cylinder was 200, 220, and 235°C, respectively, and the nozzle temperature was 230°C. The injection pressure of 10 MPa and injection speed of 60 mm/s were used.

### Compression molding

The extrudate granules of UHMWPE/PP(80/20) blends were compression molded in a press to achieve 1 and 4 mm thick plates. The blends were first preheated for 10 min at atmosphere at 190 ~ 200°C, then compressed for 10 min at 10 MPa at 190 ~ 200°C followed by another 10 min at the same pressure at room temperature. The samples for the mechanical tests were cut from the plates.

### Characterization

Stress-strain curves and the tensile strength were measured on an Instron 4302 Tensile Tester (Instron Corp., Canton, MA) according to GB 1040-79 with a crosshead speed of 100 mm/min. Izod impact strength was measured on an XJ-40A impact tester (Chengde Precision Testing Machine Co., Chengde, China) according to GB 1843-80.

The microstructure was characterized with a JSM 5900 LV scanning electron microscope (SEM). Specimens came from the impact test bars. Both the brittle fractured surface and the impact fractured surface from the injection-molded bar and compression-molded bar were observed. Generally, the brittle fractured surface was in the 1–2 Plane and the impact fractured surface the 2–3 Plane if 1 is the direction of flow, 2 the thickness direction, and 3 the transverse-wide direction for the injection-molded bar (as seen in Fig. 2). Those of compression-molded bar were prepared in the similar locations. The microstructure was also observed by polarized light microscope (PLM) in a Leitz Diaplan microscope with transmitted light. The sections in the 2–3 Plane with average thickness of 40  $\mu\text{m}$  were cut with the microtome adjacent to the notch.

The composition of the skin and core region of the test bar molded both by injection and compression molding was characterized with Fourier transform-



**Figure 2** Schematic diagram of the fractured surfaces. (1 is the direction of flow, 2 the thickness direction, and 3 the transverse-wide direction).

infrared spectroscopy (FTIR), wide angle X-ray diffraction(WAXD), and differential scanning calorimeter (DSC) analyses. The skin layer specimen and the core layer specimen were separated carefully with a fresh razor, of which a part was used for DSC analysis directly and the other was heat-pressed into thin films for FTIR and WAXD analyses. FTIR, WAXD, and DSC experiments were conducted on a NICOLET-560 FTIR Instrument in transmission mode, a Philips X'pert pad diffractometer with Cu-K $\alpha$  radiation and a NETZSCH 204 calorimeter separately.

## RESULTS AND DISCUSSION

### Mechanical properties

The typical stress-strain curves of the injection and compression-molded UHMWPE/PP(80/20) blends were shown in Figure 3. For the injection-molded part, the stress decreased with the increase of the strain from the yield point to the break. Its strength at break was lower than the yield strength. Different tensile behavior for the compression-molded part can be seen from Figure 3. Strain-hardening appeared early after yield without apparent yield

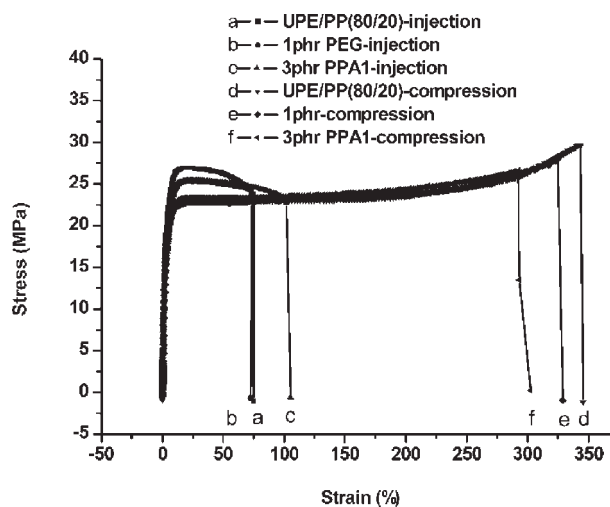


**Figure 3** Typical stress-strain curves of injection-molded and compression-molded UPE/PP(80/20)blends. (UHMWPE was abbreviated to UPE in all the figures and tables of this article).

**TABLE I**  
**Mechanical Properties of UPE/PP Blends Molded by Injection Molding and Compression Molding**

Samples	Molding condition	Young's modulus (MPa)	Yield strength (MPa)	Elongation at break (%)	Strength at break (MPa)	Impact strength (kJ/m <sup>2</sup> )
UPE/PP (80/20)	Injection	1044.0 ± 78.3	27.0 ± 0.5	67.4 ± 3.4	23.6 ± 0.5	38.6
	Compression	811.2 ± 75.3	22.9 ± 0.7	344.2 ± 18.0	30.8 ± 0.9	99.2
UPE/PP/PEG (80/20/1)	Injection	1166.0 ± 73.4	25.4 ± 0.4	65.3 ± 4.1	23.5 ± 0.4	22.6
	Compression	709.9 ± 71.8	23.2 ± 0.3	322.0 ± 6.8	27.7 ± 0.7	83.1
UPE/PP/PPA1 (80/20/3)	Injection	1017.0 ± 74.7	25.3 ± 0.3	74.2 ± 4.6	22.7 ± 0.4	26.4
	Compression	884.8 ± 74.6	23.4 ± 0.2	306.2 ± 7.2	27.6 ± 0.8	72.7

drop, with a higher strength at break than the yield strength. The tensile properties and the impact strength were summarized in Table I. For every sample, more than five specimens were tested and the average value was reported. The Young's modulus and the yield strength of the injection-molded part were obviously higher than those of compression-molded part while the elongation at break of the injection-molded part was much lower than that of compression-molded part. In the case of impact strength, the value of the injection-molded part was less than half of the compression-molded part.

The difference in the tensile properties and impact strength could result from several factors such as the blend morphology, composition distribution, and crystallinity developed during molding operation. In the following part, UHMWPE/PP(80/20) blend was chosen as the representative of this series of blends for the morphology and composition study.

### Morphology

SEM images of the fracture surfaces of UHMWPE/PP(80/20) blend were presented in Figure 4 to Figure 7. For the injection-molded blend, the whole brittle fractured surface was not smooth, and it was composed of sets of smaller surfaces in the size of hundred microns, as shown in Figure 4. This meant that UHMWPE particles did not fuse into homoge-

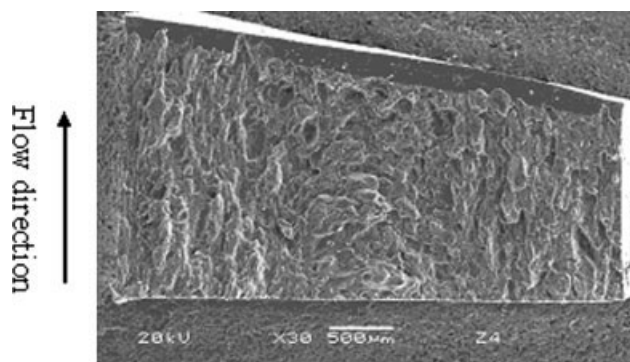


**Figure 4** SEM image of brittle fractured surface of injection molded UPE/PP(80/20) blend.

neous melt during injection molding, and the fracture was initiated and developed along the particle interfaces. Another feature in Figure 4 was that apparent skin-core structure was formed in the injection-molded UHMWPE/PP blend. In the skin region, the particles orientated in the direction of melt flow. It maybe resulted from both the flow-induced and the thermal residual stresses. Similar features also appeared in the impact fractured surface (Fig. 5). In addition, there were many cracks (shown by arrows in the figure) from the notch tip to the end of the impact fractured surface, with the big continuous crack correspondent to the boundary between the skin and the core region. In contrast, the compression molding did not form the skin-core and orientation structure in the brittle fractured surface of the UHMWPE/PP blend (Fig. 6), neither was apparent crack observed from the notch tip to the end of the impact fractured surface for the compression-molded samples (Fig. 7), though the phenomenon that fracture passed between the particles still can be seen in Figure 6 and 7.

Figure 8 showed the phase morphology of UHMWPE/PP(80/20) blend viewed by the optical microscopy using polarized light in bright field. It was more evident that UHMWPE matrix did not form homogeneous melt no matter by injection molding or compression molding. A granular structure in which UHMWPE powder particle in the size

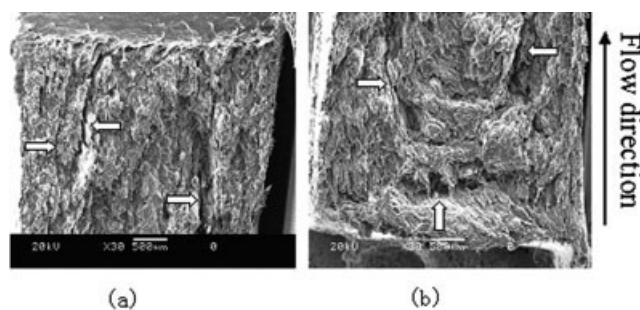


**Figure 5** SEM images of impact fractured surface of injection-molded UPE/PP(80/20) blend (arrowed inside the pictures are cracks). (a) Near the notch tip (b) near the end of the fracture surface.

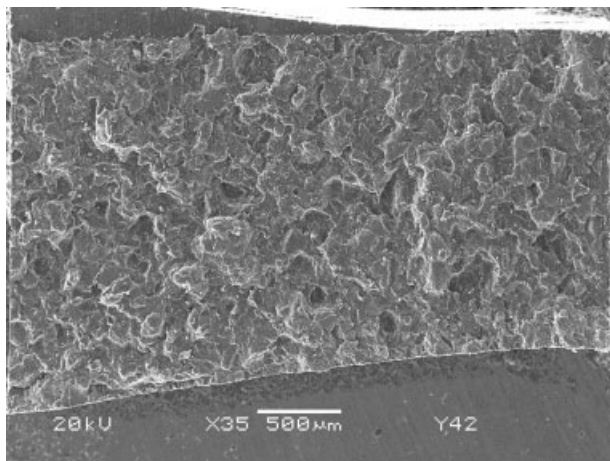


**Figure 6** SEM image of brittle fractured surface of compression-molded UPE/PP(80/20) blend.

~ 100 μm was retained. PP (with darker color in these images) seemed to distribute between UHMWPE particles in the size of micron to decamicon. Some distinguishable features also existed in the injection-molded part. A skin-core structure was apparent in the injection-molded sample, which UHMWPE particles accompanied with fused PP elongated highly in the skin and the orientation was much weakened in the core, whereas the phase morphology of the compression molded part was isotropic from the skin to the core section. Another difference between the two samples lay in the degree of consolidation. The compression molded

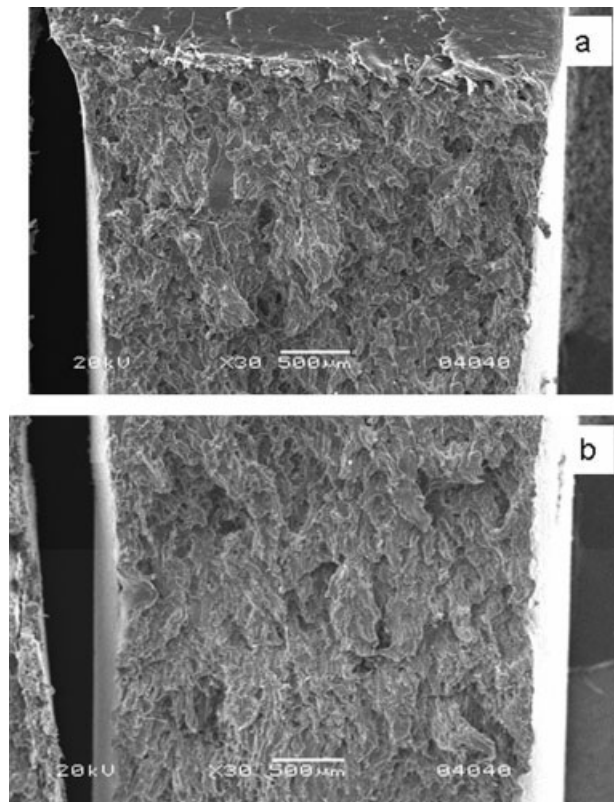


**Figure 7** SEM images of impact-fractured surface of compression-molded UPE/PP(80/20) blend. (a) Near the notch tip (b) near the end of the fracture surface.

part consolidated better than the injection one. In the injection-molded part the grain boundaries were sharp and well defined, whereas in compression

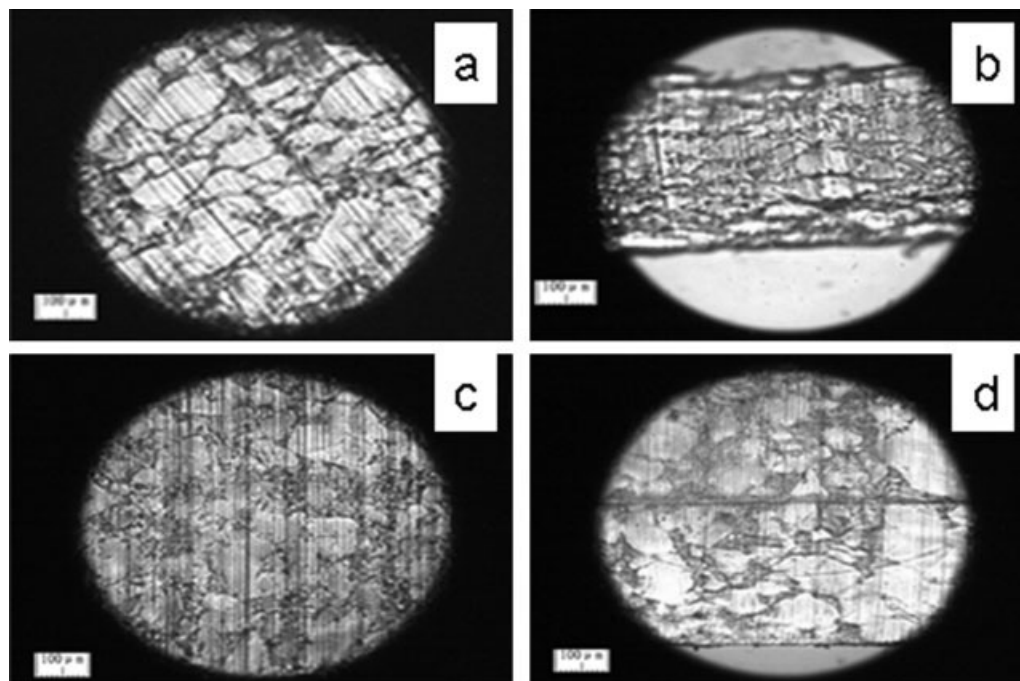


**Figure 8** Polarized light micrographs of UPE/PP(80/20) sample. (a) core section of injection sample, (b) skin section of injection sample, (c) core section of compression sample, and (d) skin section of compression sample.

molded part they were much less distinct. In fact, weak bond was so obvious in the injection-molded part that the microtome sections disintegrated in the skin region, especially in the interface between the core and the skin.

SEM and optical microscopy revealed that UHMWPE/PP blend molded by both injection and compression molding did show, to a greater or less degree, a memory of the original powder particles in the microstructure. It was reported that this memory usually formed the fuse defect in UHMWPE melt<sup>17</sup> and its severity would decrease with the increase of time, temperature and pressure during molding.<sup>18,20,21</sup> Gao and Mackley<sup>15</sup> studied the retention of powder memory in UHMWPE melt. They pointed out that to form a continuum in the melt, two conditions must be met. Firstly, adjacent faces of powder particles must be in intimate contact, and secondly, polymer chains must interfuse across this boundary. The first process was controlled largely by the applied pressure and the melt viscosity. The chain diffusion process was controlled by reptation which time varied with weight-averaged molecular mass to the power of 3.4. It was estimated that polyethylene with molecular mass of  $2 \times 10^6 \text{ kg mol}^{-1}$  needed only  $10^{-7} \sim 1\text{s}$  to ensure contact in a pressure of 40 bar and a temperature of 180°C, but the reptation time would be as long as proximately  $10^6\text{s}$ .<sup>15</sup> So it was inevitable that the degree of interface erasure would be incomplete even if UHMWPE was compression molded in 100 bar and 200°C for 10 min. Compared with compression molding, the annealing time in the mold was much shorter and the mold temperature was much lower for the injection molding. The diffusion of polymer chains therefore was less complete and much distinctive boundaries were retained in the injection molded UHMWPE/PP blend. Fracture most probably initiated and propagated from these defects when the samples were impacted. The more serious was the fuse defects, the lower impact strength might be led to. Besides the inevitable fuse defects, there were also other weak points in the injection-molded specimen, such as the skin-core interface and micro-weldlines resulted from the jetting flow during mold filling (in our investigation, we found the mold filling of tensile samples was in a laminar flow pattern and that of impact samples was in a jetting flow pattern). These stress concentration points together with the more serious fuse defects would account for the inferior resistance to impact for the injection-molded blend. In addition, the existence of the orientation structure may result in the decreased impact strength in the nonorientation direction for the injection-molded specimen.

The improvement in the small-strain tensile properties for the injection-molded blend, such as

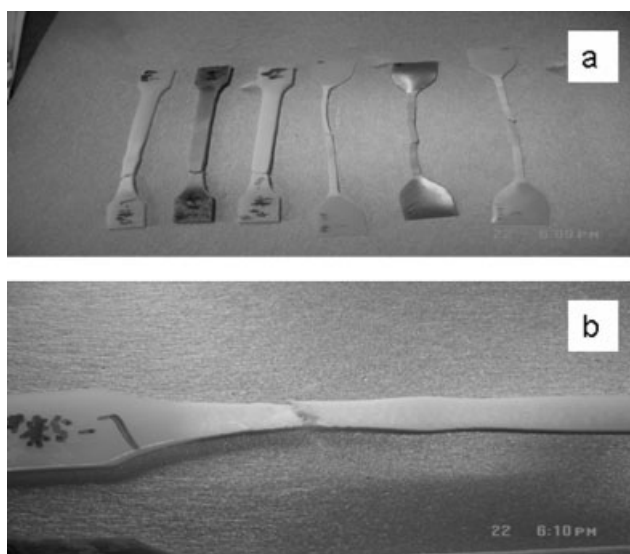


**Figure 9** Picture of broken specimen of UPE/PP(80/20) blends: (a) the left three: injection molding, the right three: compression molding (b) injection molding.

Young's modulus and yield strength, would be attributed to the skin-core structure in which the elongated particles in the skin would act as reinforcing fibers. However, the tensile behavior at large deformation, namely ultimate elongation and break strength, was influenced mainly by the increased stress concentration points and the worse consolidation state.

Figure 9 presented the appearance of the broken samples after tensile test. For the compression-molded one, the whole test zone were elongated and deformed evenly without necking behavior. The stretched zone looked smooth and whitened while the gripped section was transparent. It showed that chain orientation and stretch-induced crystallization occurred in the test zone during elongation. For the injection-molded one, necking first took place at one or two points in the test zone, and subsequently the specimen was stretched to break after the necking close to the nongate end spread a bit out. The surface in the test zone of the broken sample was coarse, covered with a lot of crazes perpendicular to the draw direction. This indicated that the injection-induced orientated particles enhanced yield strength, and the poor interfacial bonding was influential to the ultimate break.

#### Composition of skin-core structure

Generally, injection-molded immiscible polymer blends with a deformable minor phase would form skin-core morphology and orientation of the dispersed phase through out the thickness of a molded part. In the meanwhile, a distribution of the dispersed phase concentration from the core to the skin

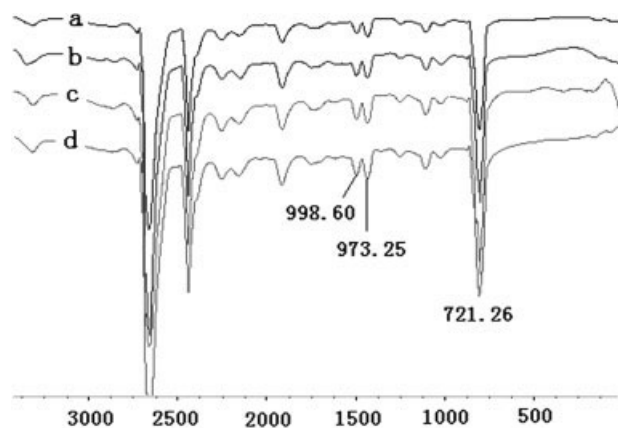


**Figure 10** FTIR spectra of the skin layer and core section of UPE/PP(80/20). (a) skin layer of injection sample, (b) core section of injection sample, (c) skin layer of compression sample, and (d) core section of compression sample.

is usually found in the injection molded blends.<sup>12,14</sup> This effect was attributed to the existence of a concentration gradient due to crystallization of the front in contact with the mold surface. However, it was also reported<sup>24</sup> that the apparent absence of dispersed phase as observed by SEM was attributed to the very fine size of the dispersed phase in the skin relative to the core and in fact both matrix and dispersed phase presented in the surface region approximately as in the original blend when revealed by detailed compositional analysis such as DSC and XPS. Whether the composition variation exists in the skin-core structure of the injection-molded UHMWPE/PP blend was another subject of our investigation in this article. In detail, the skin-core structure composition of the injection-molded part was characterized by FT-IR, DSC and WAXD, comparing with the compression-molded one.

Figure 10 showed the FTIR spectra of the skin and core section of UHMWPE/PP(80/20) blend molded by injection and compression, respectively. The absorbance bands around  $970\text{ cm}^{-1}$  are associated with  $[\text{CH}_2\text{CH}(\text{CH}_3)]_n$  of PP, and the bands around  $720\text{ cm}^{-1}$  are associated with  $[\text{CH}_2]_n$  ( $n > 4$ ) of UHMWPE. The ratios of the absorbance bands area of PP ( $A_{970}$ ) to that of UHMWPE ( $A_{720}$ ) are used to denote the relative content of PP and UHMWPE, as

**TABLE II**  
Relative Absorbance of the Skin and Core Section of UPE/PP(80/20) Specimens Obtained from Injection Molding and Compression Molding

Molding condition	$A_{970}/A_{720}$	
	Skin-section	Core-section
Injection	0.1874	0.1832
Compression	0.1935	0.2080

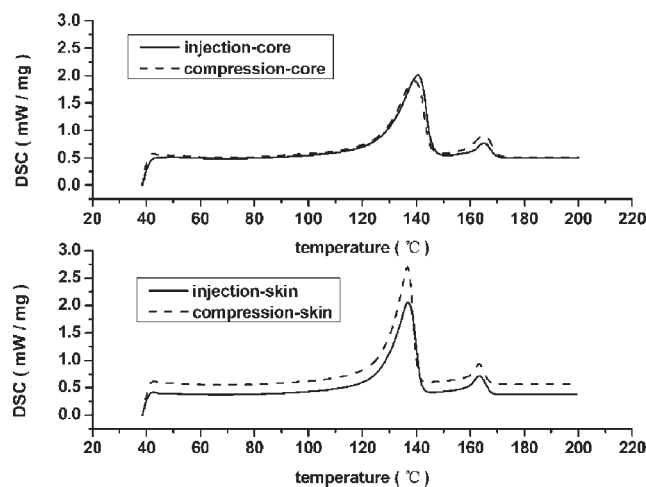


**Figure 11** DSC curves of the skin and core sections of UPE/PP(80/20) specimen from injection molding and compression molding.

shown in Table II. For injection-molded sample, there was a little more PP in the skin than in the core. And the case was opposite for the compression-molded sample. In fact, the difference of PP content analyzed by FTIR between the skin and core section was very small for both molded parts.

In the DSC thermograms (Fig. 11), the melting peak, appearing at  $137^\circ\text{C}$ , corresponds to the melting of crystallized UHMWPE, and the peak at  $164^\circ\text{C}$  is attributed to the melting of crystallized PP in the UHMWPE/PP blend. Assuming that the crystallization of UHMWPE and PP did not interfere with each other, the relative content of PP in the specimens could be denoted by the ratio of PP crystal melting enthalpy ( $\Delta H_{\text{PP}}$ ) to that of UHMWPE ( $\Delta H_{\text{UHMWPE}}$ ), which were summarized in Table III. The results indicated that the skin section contained more PP than the core section for the injection-molded specimen and the case was opposite for the compression-molded specimen, which is consistent with the results of FTIR analysis.

The WAXD pattern of the specimen was shown in Figure 12. It can be seen that four peaks at  $13.9$ ,  $16.7$ ,  $21.4$ , and  $23.9^\circ$ , corresponding to the reflections of [110] and [040] Planes of  $\alpha$ -PP and [110] and [200] Planes of UHMWPE appeared in all the skin and core specimens. The relative intensities of [110] and

**TABLE III**  
DSC Data of the Different UPE/PP(80/20) Specimens

Samples	$\Delta H_{\text{UPE}}$ (J/g)	$\Delta H_{\text{PP}}$ (J/g)	$\Delta H_{\text{PP}}/\Delta H_{\text{UPE}}$ (%)
Injection-skin	112.1	11.5	0.1029
Injection-core	123.5	10.6	0.0859
Compression-skin	129.0	11.9	0.0925
Compression-core	111	18.5	0.1670

[040] diffraction peaks of  $\alpha$ -PP to that of the [110] Plane of UHMWPE were listed in Table IV. For the injection molded sample, the relative intensity of [110] and [040] diffraction peaks of  $\alpha$ -PP to that of the [110] Plane of UHMWPE in the skin section was higher than that in the core section, indicating that more PP was distributed in the skin. Opposite case occurred to the compression-molded sample, with less PP contained in the skin and more PP in the core.

From the results of FT-IR, DSC, and X-ray diffraction another difference between the injection-molded UHMWPE/PP blend and compression one was revealed that there was more PP in the skin than core for the injection-molded part, while less PP was found in the skin than core for the compression-molded part. It may also be one of the reasons that two types of molded part behaved differently in mechanical properties. Although the elongated UHMWPE particles in the skin improved the tensile properties of injection-molded UHMWPE/PP blend in small strain, namely Young's modulus and yield strength, weakened bonding resulted from more PP which is immiscible with UHMWPE would lead to slip and crack more easily between UHMWPE particles after yielding, especially in the direction perpendicular to the orientation direction (also the draw direction during tensile testing). This was why many crazes perpendicular to the draw direction can be seen in the appearance of injection-molded sample. The breaking of the skin section would increase the stress sharply for the whole sample and failure occurred quickly. In compression-molded part, there was no reinforcing particles of oriented UHMWPE and less PP in the skin section, the external stress was distributed and transferred evenly in the sample

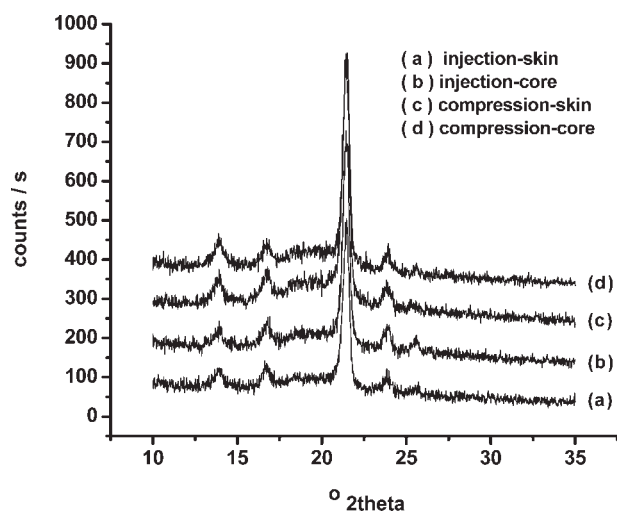


**Figure 12** WAXD patterns of the skin and core section of UPE/PP(80/20) specimen from injection molding and compression molding.

**TABLE IV**  
Relative Intensity (%) of [110]-[040] of  $\alpha$ -PP with [110] of UHMWPE in Different UHMWPE/PP(80/20) Specimens

	[110] of $\alpha$ -PP $2\theta = 13.9^\circ$	[040] of $\alpha$ -PP $2\theta = 16.7^\circ$	[110] of UPE $2\theta = 21.4^\circ$
Injection-skin	9.72	11.14	100
Injection-core	6.77	8.41	100
Compression-skin	11.06	12.72	100
Compression-core	16.00	13.94	100

during stretching, so the specimen deformed evenly in the entire tested zone, causing orientation and recrystallization.

The difference in crystallinity of the blend between two molding operations could be estimated roughly from the melting enthalpies of UHMWPE and PP presented in Table III. The compression-molded part has slightly higher crystallinity than the injection molded one. Generally speaking, higher crystallinity would lead to higher Young's modulus and yield strength, and lower impact strength. The fact that the compression-molded part with higher crystallinity had relatively lower Young's modulus and yield strength, and much higher impact strength than the injection one might mean that the difference in crystallinity resulted from the two molding operations was much less influential to the mechanical properties, compared with that of morphology and composition distribution.

## CONCLUSIONS

By blending with polypropylene(PP), ultrahigh molecular weight polyethylene(UHMWPE) can be processed by conventional injection as well as compression molding. Two molded parts of UHMWPE/PP(80/20) blend behaved differently in mechanical properties. The young's modulus and yield strength of the injection molded blend were obviously higher than those of compression-molded one while the elongation at break and impact strength of the injection-molded part were much lower than those of compression-molded one. No strain hardening effect occurred to injection-molded bar during tensile test, with lower strength at break than the yield strength. And opposite case occurred to the compression-molded one.

The mechanical behavior was thought to relate with the phase morphology formed in molding operation. Both SEM and optical microscopy were used in the morphological study. For the injection-molded blend, an apparent skin-core structure was observed in all brittle fractured surfaces, impact fractured surface and microtome section, in which the



UHMWPE particles elongated highly in the skin and the orientation was much weakened in the core. In the compression-molded part, the phase morphology was isotropic from the skin to the core section. The difference of consolidation degree between two molded parts, that the compression molded part consolidated better than the injection one, was also clearly shown in the SEM and Polarized light micrographs.

In addition, composition variation was found to exist in the skin-core structure of the injection-molded UHMWPE/PP blend. Results of FTIR, DSC, and WAXD analyses all indicated that there was more PP in the skin than core for the injection-molded part, whereas less PP was found in the skin than core for the compression-molded part. It may also be one of the reasons that two molded parts behaved differently in mechanical properties.

## References

1. Bhateja, S. K.; Andrews, E. H. *Polym Eng Sci* 1983, 23, 888.
2. Kyu, T.; Vadhar, P. *J Appl Polym Sci* 1986, 32, 5575.
3. Tincer, T.; Coskun, M. *Polym Eng Sci* 1993, 33, 1243.
4. Liu, G. D.; Chen, Y. Z.; Li, H. L. *J Appl Polym Sci* 2004, 94, 977.
5. Aiello, R.; La Mantia, F. P. *Macromol Mater Eng* 2001, 286, 176.
6. Utsumi, M.; Nagata, K.; Suzuki, M.; Mori, A.; Sakuramoto, I.; Torigoe, Y.; Kaneeda, T.; Moriya, H. *J Appl Polym Sci* 2003, 87, 1602.
7. Liu, G. D.; Li, H. L. *J Appl Polym Sci* 2003, 89, 2628.
8. Liu, G. D.; Xiang, M.; Li, H. L. *Polym Eng Sci* 2004, 44, 197.
9. Xie, M. J.; Liu, X. L.; Li, H. L. *J Appl Polym Sci* 2006, 100, 1282.
10. Xie, M. J.; Li, H. L. *Eur Polym Mater* 2007, 43, 3480.
11. Ghiam, F.; White, J. L. *Polym Eng Sci* 1991, 31, 76.
12. Karger-Kocsis, J.; Csikai, I. *Polym Eng Sci* 1987, 27, 241.
13. Li, Z. M.; Yang, W.; Yang, S. Y.; Xie, B. H.; Huang, R.; Yang, M. B.; Feng, J. M. *J Mater Sci* 2004, 39, 413.
14. Fellahi, S.; Favis, B. D.; Fisa, B. *SPEANTEC Tech Pap* 1993, 39, 211.
15. Gao, P.; Mackley, M. R. *Polymer* 1994, 35, 5210.
16. Farrar, D. F.; Brain, A. A. *Biomaterials* 1997, 18, 1677.
17. Wu, J. J.; Buckley, C. P.; O'Connor, J. J. *J Mater Sci Lett* 2000, 20, 473.
18. Wu, J. J.; Buckley, C. P.; O'Connor, J. J. *Biomaterials* 2002, 23, 3773.
19. Gul, R. M.; McGarry, F. *J Polym Eng Sci* 2004, 44, 1848.
20. Parasnis, N. C.; Ramani, K. *J Mater Sci Mater Med* 1998, 9, 165.
21. Gao, P.; Chueng, M. K.; Leung, T. Y. *Polymer* 1996, 37, 3265.
22. Jauffres, D.; Lame, O.; Vigier, G.; Dore, F. *Polymer* 2007, 48, 6374.
23. Wang, Z. G.; Hsiao, B. S.; Stribeck, N.; Gehrke, R. *Macromolecules* 2002, 35, 2200.
24. Fellahi, S.; Favis, B. D.; Fisa, B. *Polymer* 1996, 37, 2615.